



Cold-spray coating of an Fe-40 at.% Al alloy with additions of ruthenium

by R.A. Couperthwaite*, L.A. Cornish^{†‡} and I.A. Mwamba*

Synopsis

In previous work by the authors, it was established that additions of 0.2 at.% Ru to an Fe-40 at.% Al alloy improved the corrosion and oxidation resistance of the alloy. The alloy was produced by mechanical alloying and spark plasma sintering and the work showed that non-equilibrium processing was able to significantly refine the grain size of the material. The sintered material had a higher hardness than the as-cast material and the change in grain size did not significantly affect the oxidation and corrosion. In the present research, the mechanically alloyed powder was coated onto a mild steel substrate using cold-spray coating at a gas pressure of 10 bar and a temperature of 500°C. The coatings were found to be 5–10 µm thick, although thicknesses of up to 30 µm were observed. The coated materials were subjected to oxidation and corrosion tests to determine the effectiveness of the coating in increasing the oxidation and corrosion resistance of mild steel. This was done to determine the effectiveness of cold-spray coating as a technique to coat these mechanically alloyed powders.

Keywords

Fe-Al alloy, mechanical alloying, cold-spray coating, addition, corrosion resistance.

Introduction

Previous work conducted by Mintek (Couperthwaite *et al.*, 2013, 2015) investigated the effect of precious metal additions on the structure, oxidation and corrosion properties of an Fe-40 at.% Al (Fe-Al) alloy. Initial work determined that additions of more than 0.5 at.% precious metal did not improve the oxidation and corrosion properties of the materials and in some cases even decreased the resistance to corrosion. Further work identified Pt and Ru as beneficial additions to the FeAl alloy. Four alloys were then produced by mechanical alloying and sintering (FeAl-0.2 at.% Pd, FeAl-0.2 at.% Ru, FeAl-0.5 at.% Ag, FeAl-0.5 at.% Pt). These alloys were all successfully produced by melting and casting and mechanical alloying sintering and it was found that the non-equilibrium processing greatly decreased the grain size of the materials compared to the as-cast materials. It was found that the additions of Ru and Pt were still the most beneficial to the oxidation and corrosion properties, with Ru being considered the most beneficial.

This report details the results from the initial spray testing work done with the FeAl-0.2 at.% Ru alloy powder produced by mechanical alloying. There are several options for powder coating onto substrates; thermal-spray techniques, which include high-velocity oxy-fuel (HVOF) coating and plasma coating, or cold-spray (also known as supersonic-spray) techniques. Cold-spray techniques have attracted a lot of interest lately and as a system is available at University of the Witwatersrand, it was decided to use cold spraying in the current work. This work was done to determine the effectiveness of cold-spray coating of these mechanically alloyed powders.

Fe-Al Alloys

The iron-aluminium system has attracted a large amount of research due to the fact that Fe-Al intermetallic compounds possess good mechanical properties, along with low density and low cost, as well as easy access to the raw materials (Ji *et al.*, 2006; Montealegre *et al.*, 2000). Arzhnikov *et al.* (2008) found that the Fe-Al alloys are promising, due to their good refractoriness, oxidation and corrosion resistance and good ductility at room temperature. In comparison to conventional alloys, Fe-Al alloys perform much better at higher temperatures, due to the stability of the

* Advanced Materials Division, Mintek, Randburg, South Africa.

† School of Chemical and Metallurgical Engineering, University of the Witwatersrand, Johannesburg, South Africa.

‡ Centre of Excellence in Strong Materials, University of the Witwatersrand, Johannesburg, South Africa.

© The Southern African Institute of Mining and Metallurgy, 2016. ISSN 2225-6253. This paper was first presented at the AMI Ferrous and Base Metals Development Network Conference 2016 19–21 October 2016, Southern Sun Elangeni Maharani, KwaZulu-Natal, South Africa.

Cold-spray coating of an Fe-40 at.% Al alloy with additions of ruthenium

microstructure originating from the low diffusivity of Fe in Al (Nayak *et al.*, 2010). However, the Fe-Al alloys are difficult to fabricate in bulk, due to their poor castability and workability (Zhu *et al.*, 2009); this was confirmed by Kuc *et al.* (2009) who found that Fe-Al alloys have an activation energy for deformation of 484.9 kJ/mol compared to 392 kJ/mol for austenitic steel. The region of interest in the current study is the Fe-Al intermetallic compound at around 60 at.% Fe (Figure 1), which is a single-phase bcc region (Eelman *et al.*, 1998).

Mechanical alloying

During mechanical alloying, fine particles are cold-welded together to form larger particles. Once the particles become too large, the milling process breaks them into smaller particles. These two processes continue until the powder has a single uniform composition.

Several studies exist on the processing of Fe-Al alloys by mechanical alloying and mostly the conditions of the milling were different. Nayak *et al.* (2010) used toluene as a process control agent (PCA) and full solid solution of Fe in Al was found after 20 hours' milling at 300 r/min. It was also found that the hardness had improved, due to the nanocrystalline Fe₄Al₁₃ intermetallic compound formed, the absence of the soft Al phase and the large number of defects induced during mechanical alloying. Skoglund *et al.* (2004) produced an Fe-40 at.% Al alloy by milling with a stearic acid PCA for 4 hours at 360 r/min and created an alloy containing mostly FeAl with some Fe₃Al. Song *et al.* (2009) worked on a nearly equiatomic Fe-Al alloy and milled the powders for 3 to 12 hours at 304 r/min with ethanol as the PCA. After milling, the powder was annealed at 1100°C in a vacuum. Their results indicated that FeAl had not formed by the end of the 12 hours of milling, but that FeAl was formed in the powder after annealing. Abhik *et al.* (2008) found that it was possible to produce FeAl after 10 hours of milling with toluene as a PCA. Shi *et al.* (2008) investigated the stages in

which the alloy forms during the mechanical alloying process. They milled the powders for a total of 50 hours and found that initially the powder formed a solid solution of Al in Fe and as milling time increased, the phase changed to the B2 FeAl phase. After 30 hours of milling the powder consisted of only B2 FeAl.

Another critical parameter that was varied greatly in these studies was the ball to powder ratio. Ratios from as low as 4:1 (Skoglund *et al.*, 2003) to as high as 15:1 (Kezrane *et al.*, 2012), 20:1 (Cheng *et al.*, 2006), 30:1 (Ko, 2010) and 50:1 (Haghighi *et al.*, 2010) were used, although most researchers used a ball-to-powder ratio of 8:1 (Krasnowski *et al.*, 2002, 2006; D'Angelo *et al.*, 2009; Abhik *et al.*, 2008).

Research has already been done on the production of a nanocrystalline coating of the Fe-40Al alloy using spray coating (Grosdidier, 2001), which successfully created a coating with a nanocrystalline grain structure with the milling structure of the feed powders retained in the final coating. There was a problem with the presence of some oxides and depletion of the aluminium content as a result of the thermal spraying. Valdrè *et al.* (1999) and Skoglund *et al.* (2003) found that there was oxygen in the final compacts after mechanical alloying and this was attributed to oxygen present in the aluminium feed powder. Several research teams have successfully created nanocrystalline FeAl materials through mechanical alloying, with crystallite sizes of 10 nm (Valdrè *et al.*, 1999) and 23 nm (D'Angelo *et al.*, 2009, Krasnowski and Kulik, 2007a, 2007b).

Oxidation of Fe-Al alloys

During oxidation testing of Fe-Al alloys a 'wrinkling' of the oxide layer has been observed. All binary Fe-Al alloys experience this effect when subjected to oxidation at temperatures of 900–1100°C (Yang *et al.*, 2005). This wrinkling effect has been attributed to high thermal stresses during cooling of the alloy (Montealegre *et al.*, 2000) and it was

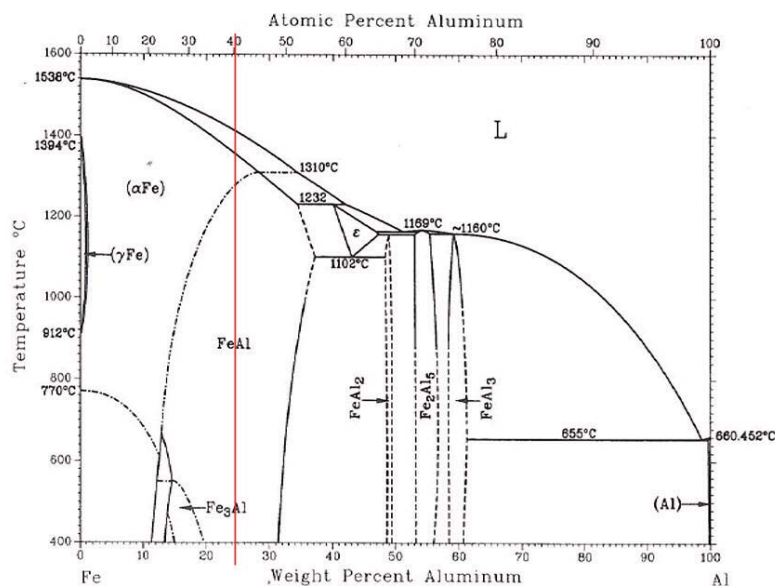


Figure 1—Fe-Al phase diagram (Massalski, 1990)

Cold-spray coating of an Fe-40 at.% Al alloy with additions of ruthenium

suggested that slow cooling retarded, or even completely prevented, the effect. Xu *et al.* (2001) found that adding Y to the Fe-Al alloys can reduce or prevent the wrinkling and spallation of the oxide layer. Xu *et al.* (2000) investigated the reasons for the weaker oxidation resistance of Fe-Al alloys in air compared to pure oxygen and found that at 1100°C in air, the Fe-Al alloys produced a mixed layer of Al₂O₃ and AlN between the outer Al₂O₃ layer and the metal

Guo *et al.* (2011) found that an Fe-Al coating applied to a 316 stainless steel substrate formed a good bond with the substrate and imparted good oxidation resistance to the metal, due to the formation of a dense and adherent oxide film. Nowak and Kupka (2012) investigated the oxidation of an Fe-Al alloy with additions of B, Cr and Zr and found that the stable α -Al₂O₃ oxide layer started forming at around 900°C. Below this temperature, unstable γ - and θ -type oxides formed. Grabke (1999) concluded that although FeAl contains a high percentage of aluminium, it does not have as good an oxidation resistance as would be expected, due to the formation of transient oxide forms at temperatures below 1000°C.

However, Paldey *et al.* (2003) found that an FeAl coating on 440C stainless steel reduced the mass gain during oxidation tests at 800°C by four times and the same coating on a 304 stainless steel reduced the mass gain by an order of magnitude. Airiskallio *et al.* (2010) and Xu *et al.* (2000) found that additions of Cr (Airiskallio *et al.*, 2010) or a combination of Y and Zr (Xu *et al.*, 2000) to the alloy helped the oxidation resistance, although additions of only Zr decreased the oxidation resistance (Xu *et al.*, 2000).

Cold-spray coating

Cold-spray coating is a technique that was first developed in the mid-1980s. This technique utilizes temperatures significantly below the melting point of the metal being coated –

typically below 1000°C (Concstell *et al.*, 2015). In order to achieve deposition of the material it is necessary to use very high impact velocities and as a result, cold-spray systems also use very high gas pressures (Grigoriev *et al.*, 2015). Recently, there has been increased interest shown in cold-spray coatings and numerous materials have been used as coatings. Some of these materials and the conditions for the coating work are shown in Table I.

Several authors found that cold-spraying of the powders maintained the powder microstructure in the sprayed coating (Jan *et al.*, 2015; Luo and Li, 2012). It was also found that cold-spraying was able to produce coatings with less oxidation than thermal spraying processes (Concstell *et al.*, 2015; Aghasibeig *et al.*, 2016). As shown in Table I, the parameters for the spray coating vary significantly, even for the targeted Fe-Al alloys.

Experimental procedures

Mechanical alloying

The milling was done on a Retsch PM100 milling machine with a stainless steel milling pot and stainless steel balls of two sizes (Table II). The milling was done for the entire time

Table II

Mechanical alloying parameters

Parameter	Value	Parameter	Value
Ball to powder ratio	10:1	Process control agent (wt.%)	0.5
Ball mass (g)	500 g (20 mm) + 500 g (10 mm)	Speed (r/min)	300
Powder sample mass (g)	100	Milling time (h)	24

Table I

Cold-spray parameters found in the literature

Material	Pressure (bar)	Temperature (°C)	Standoff distance (mm)	Reference
Fe-Cr-Si-B-C	40	700–900	30–50	Concstell <i>et al.</i> , 2015
304L	23.1–27.9	550	22	Coddet, Verdy, Coddet, Debray, <i>et al.</i> , 2015
Ag-Cu	23–30	500	20	Coddet, Verdy, Coddet and Debray 2015
Fe-40 at.% Al	30–40	800–1000	-	Cinca <i>et al.</i> , 2015
TiO ₂	9	600	-	Buhl <i>et al.</i> , 2015
Ni	30–50	800–1000	25	Aghasibeig <i>et al.</i> , 2016
Ti-Al	15	300	-	Jan <i>et al.</i> , 2015
Ni-Al	15	300	-	Jan <i>et al.</i> , 2015
Fe-Al	15	300	-	Jan <i>et al.</i> , 2015
Cu	40–50	300–600	-	Jakupi <i>et al.</i> , 2015
TiO ₂	30–40	300–900	60	Herrmann-Geppert <i>et al.</i> , 2016
Al	25–40	300–400	10–50	Henao <i>et al.</i> , 2016
NiCrAlBN	22	650	20	Luo and Li, 2015
Fe-40 at.% Al	25	550	20	Luo Li, 2012
Al	30	500	-	Kim <i>et al.</i> , 2015
Ni	38–40	650–750	40–50	Koivuluoto <i>et al.</i> , 2015
NiCu	38–40	650–750	40–50	Koivuluoto <i>et al.</i> , 2015
NiCuAl ₂ O ₃	38–40	650–750	40–50	Koivuluoto <i>et al.</i> , 2015
Ti-6Al-4V	28	520	30	Li <i>et al.</i> , 2007
Ti	28	520	30	Li <i>et al.</i> , 2007
Al	28	520	30	Li <i>et al.</i> , 2007
FeAlAl ₂ O ₃	20	500	20	Wang, Li <i>et al.</i> , 2008
FeAl	20–25	350	20	Wang, Li <i>et al.</i> , 2008
FeAl	20–25	510	15	Yang <i>et al.</i> , 2011

Cold-spray coating of an Fe-40 at.% Al alloy with additions of ruthenium

period specified, with no interval. The selected PCA was stearic acid. Powder mixing, as well as the filling and sealing of the milling pots was done in a glovebox under an argon atmosphere to reduce oxygen entrapment.

Annealing

After milling of the powders, an annealing treatment was performed to ensure that the powder was of a single phase. This annealing was done in a horizontal tube furnace under an argon atmosphere to prevent oxidation of the powders. Annealing conditions are shown in Table III.

Cold-spray coating

Cold spraying was done on a Centreline SST™ Series P cold-spray system using compressed air as the carrier gas. Several runs were conducted in order to determine the optimum parameters for the coating. The conditions for the various runs are shown in Table IV. Run 6 was a repeat of run 5 in order to have a second sample prepared in the same way for use in corrosion testing. The Fe-Al alloy was coated onto a mild steel substrate.

After these trial runs were completed, two more samples were coated. These samples were coated on all sides using the conditions in run 6, in order to be used later for conducting oxidation testing on the coatings. The gun was moved over the surface of the substrate blocks to ensure an even coating of the substrate.

Oxidation

Coated samples as well as an uncoated substrate sample were weighed and then placed in a muffle furnace. The furnace was heated at 10°C per minute to a temperature of 1000°C. The temperature was then kept constant for 48 hours, after which the heating was turned off and the samples were allowed to cool in the furnace to room temperature. Samples were then removed, weighed, sectioned and mounted for analysis. The samples were wrapped with copper tape prior to preparation.

Table III

Annealing parameters

Parameter	Ramp rate (°C/min)	Holding temperature (°C)	Holding time (h)	Gas pressure (kPa)
Value	10	550	2	200

Table IV

Conditions for cold-spray coating

Condition	Run 1	Run 2	Run 3	Run 4	Run 5	Run 6	Run 7
Temperature (°C)	400	500	500	500	500	500	500
Pressure (bar)	9.65	9.65	9.65	10	10	10	10
Standoff distance (mm)	10	10	10	10	10	10	10
Feed rate (%)	40	40	60	40	40	40	40
No. of passes	1	1	1	1	2	2	5

Results

Coating characterization

During the characterization of the coatings, it was found that the initial run of powder had been contaminated with nickel and as a result the coatings were a mix of FeAl, NiAl and Ni₃Al. This contaminated material will be referred to as Fe/Ni-Al. The samples were still characterized fully and the oxidation testing was done on the material as well to determine whether the addition of nickel to the mechanically alloyed material had any effect on the properties of the coating. Figure 2 shows the cross-section of the coating from Run 6 of the trial coating runs (two coating passes). The coating was quite thin, in the region of 3 μm and has a slight two-tone contrast in it showing the different phases in the coating material. The cross-section of the sample coated using five passes (run 7) is shown in Figure 3. After five passes the coating has not built up in any significant way, as the thickness was still at around 3 μm. The contrast in the coating showing the different phases was still visible.

A second run of powder was produced and care was taken to ensure that the feed powders were not contaminated. This correct alloy will be referred to as FeAl. This batch was coated onto the substrate using only the conditions for runs 6 and 7. The cross-sections of the sample coated with two and

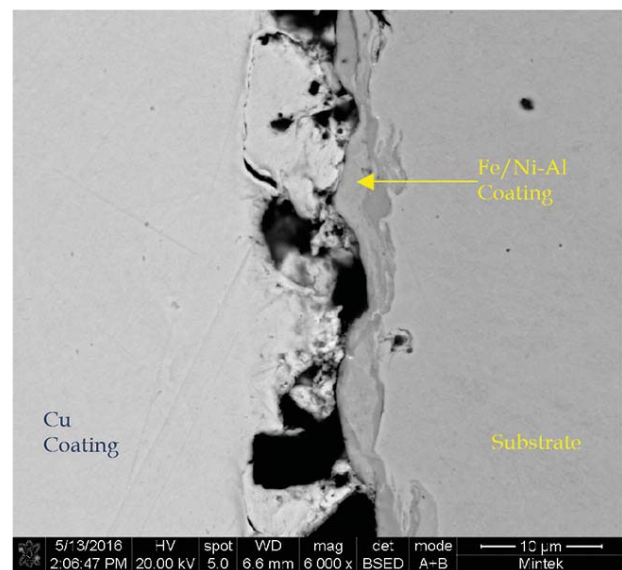


Figure 2—SEM-BSE image of the Fe/Ni-Al coating made with two passes on a mild steel substrate

Cold-spray coating of an Fe-40 at.% Al alloy with additions of ruthenium

five passes are shown in Figures 4 and 5. The coatings did not differ significantly from the Ni-containing coatings in terms of thickness. However, the different contrasts seen in the Ni-containing coatings were not observed.

With both powder lots, the thickness of the coatings obtained is a concern as it would have been preferable to have coatings of at least 10 μm in thickness. There are a number of factors that could be changed to influence this, one being the spray pressure during coating. Unfortunately the system utilized for the spray coating had a maximum pressure limit of 10 bar. Another option would be to increase the temperature used in the spray coating to the upper limit of around 800–1000°C. The third and final option would be to investigate the use of another coating technique such as high-velocity oxy-fuel (HVOF) or plasma-spray coating.

Oxidation trial

The weights of the samples before and after the oxidation treatment as well as the percentage mass increase are shown in Table V. All samples showed an increase in mass, indicating that they were oxidized. The percentage weight gain of all the samples was not significantly different and as such the coatings applied to the samples were not effective in preventing the oxidation of the mild steel.

The oxidized samples were cold-mounted, carbon coated and analysed on the SEM. As expected from the mass gain of the samples during the oxidation trial, all the samples showed significant oxide on the surface of the substrates. The oxides were too thick to be observed in a single SEM image and so only a small portion of each oxide layer is shown in the images. EDX analysis did not reveal any Al in the oxide layer, even at the very edge of the layer. As a result, it could not be determined whether the coating was still intact on top of the oxide layer for the two coated samples (Figure 6–8).

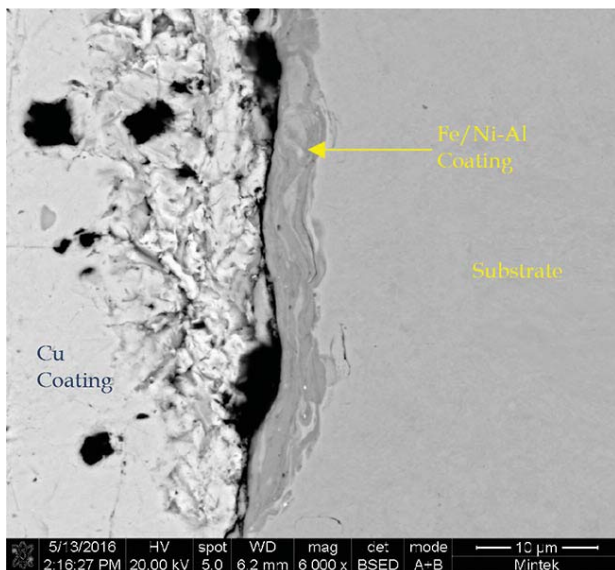


Figure 3—SEM-BSE image of the Fe/Ni-Al coating made with five passes on a mild steel substrate

The compositions of the oxide layers were analysed by SEM-EDX (Table VI). The composition was found to be consistent with the oxidation of the mild steel substrate. The

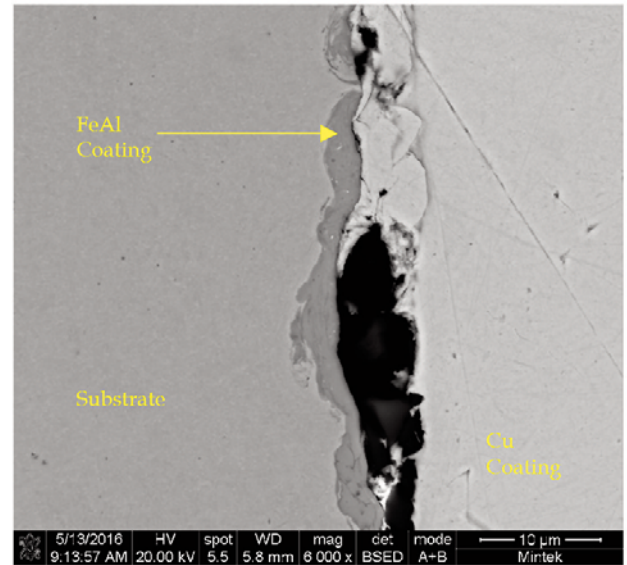


Figure 4—SEM-BSE image of the FeAl coating made with two passes on a mild steel substrate

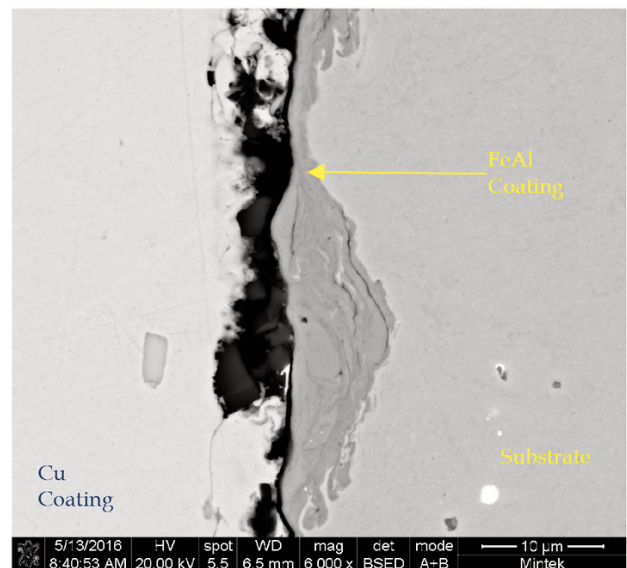


Figure 5—SEM-BSE image of the FeAl coating made with five passes on a mild steel substrate

Table V

Sample weight changes during oxidation treatment

	Mass before oxidation (g)	Mass after oxidation (g)	Weight gain (%)
Mild steel	78.534	84.501	7.6
Fe/Ni-Al	127.919	138.228	8.1
FeAl	122.906	131.452	7.0

Cold-spray coating of an Fe-40 at.% Al alloy with additions of ruthenium

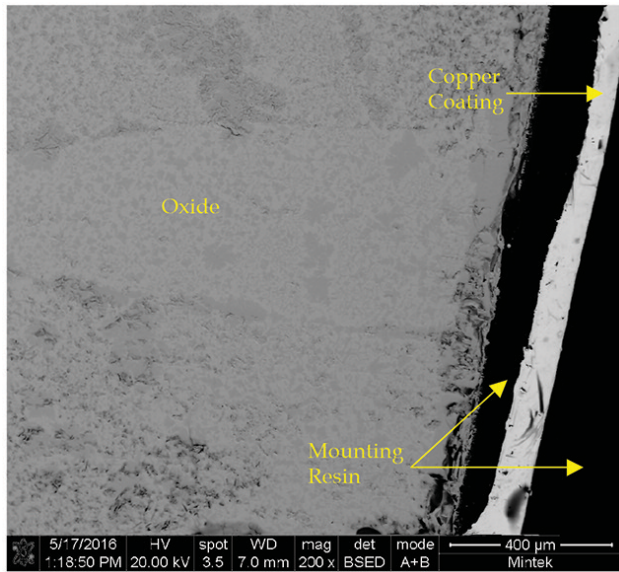


Figure 6—SEM-BSE image of the oxide layer on the uncoated mild steel sample

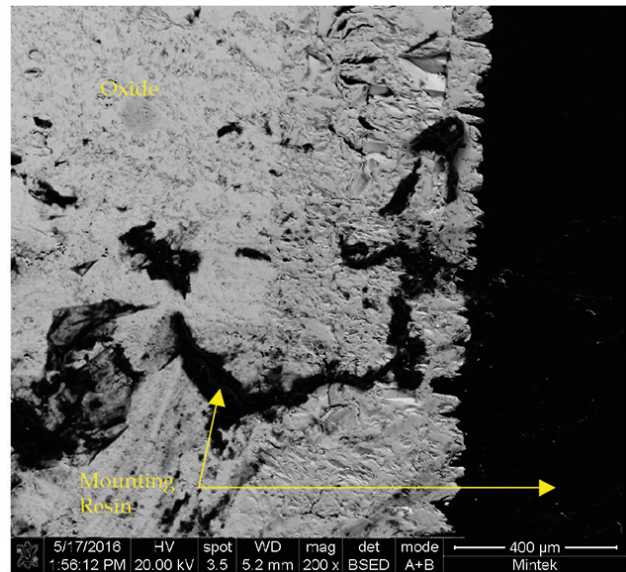


Figure 8—SEM-BSE image of the oxide layer on the sample coated with the FeAl alloy

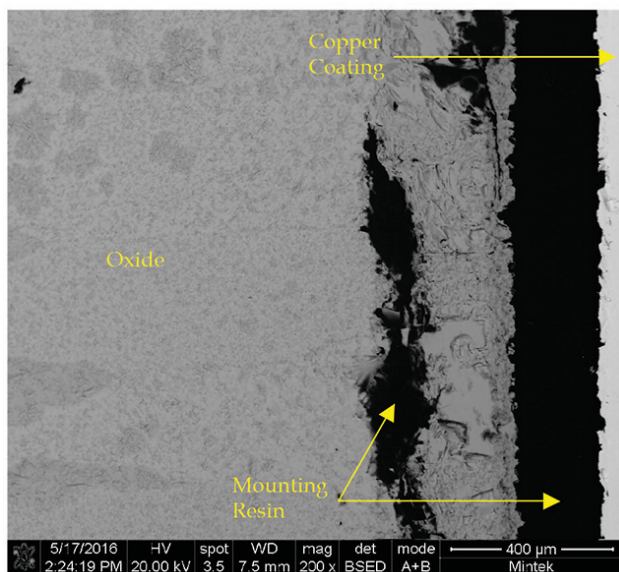


Figure 7—SEM-BSE image of the oxide layer on the sample coated with the Fe/Ni-Al alloy

oxide layers showed two contrasting regions, light and dark and these were analysed on the uncoated sample to determine whether a significant difference existed. It was found that there was a slightly higher oxygen content in the dark regions; however, the difference was not hugely significant. No evidence of the coatings was found on the oxidized samples, indicating that the coatings were ineffective at protecting the substrate.

Discussion

Cold-spray coating of the samples produced very thin coatings on the samples, around 3–5 µm. This is significantly

Table VI
EDX analysis of oxide layers after oxidation trial

At. %	Uncoated mild steel			Fe/Ni-Al	FeAl
	Light	Dark	Overall		
O	42.4±0.6	49.4±0.8	44.9±0.1	44.5±0.4	45.4±0.9
Mn	1.1±0.2	0.6±0.1	0.9±0.1	1.0±0.1	1.0±0.1
Fe	56.5±0.6	48.8±2.0	54.2±0.2	54.5±0.3	53.6±0.9
Cu		1.3±2.2			

thinner than expected and it would be preferable to have a coating thickness of 10 µm or greater. There are a number of options available for improving the deposition efficiency of the cold-spray process. The first and likely most effective option, would be to increase the pressure used during the spraying. Alternatively, it may be necessary to change the coating technique and rather use HVOF, or plasma-spray coating. The oxidation trial of the coated samples confirmed that the coating was not sufficient to protect the substrate from oxidation, as all samples oxidized significantly during the trial. Considering the performance of the coating material in oxidation trials as a bulk sintered material, it is possible that the coating was too thin, not uniform enough, or slightly porous and so allowed oxygen to penetrate to the surface of the substrate.

Conclusions

Cold-spray coating was used successfully to coat the mechanically alloyed powders onto a substrate. However, at the pressures used in this study, the coatings applied to the substrates were very thin. This resulted in a coating that was not effective at preventing the oxidation of the mild steel

Cold-spray coating of an Fe-40 at.% Al alloy with additions of ruthenium

substrates when exposed to high temperatures. As such, it will be necessary to investigate whether a higher pressure can be used in the coating process, as well as the use of alternative coating methods.

References

- ABHIK, N.C., VIVEK, R., UDHAYABANU, V. and MURTY, B.S. 2008. Influence of heat of formation of B2/L12 intermetallic compounds on the milling energy for their formation during mechanical alloying. *Journal of Alloys and Compounds*, vol. 465, no. 1–2. pp. 106–112.
- AGHASIBEIG, M., MONAJATIZADEH, H., BOCHER, P., DOLATABADI, A., WUTHRICH, R. and MOREAU, C. 2016. Cold spray as a novel method for development of nickel electrode coatings for hydrogen production. *International Journal of Hydrogen Energy*, vol. 41, no. 1. pp. 227–238.
- AIRISKALLIO, E., NURMI, E., HEINONEN, M.H., VAYRYNEN, I.J., KOKKO, K., ROPO, M. and VITOS, L. 2010. High temperature oxidation of Fe–Al and Fe–Cr–Al alloys: The role of Cr as a chemically active element. *Corrosion Science*, vol. 52, no. 10. pp. 3394–3404.
- ARZHNIKOV, A.K., DOBYSHEVA, L.V. and TIMIRGAZIN, M.A. 2008. Formation and ordering of local magnetic moments in Fe–Al alloys. *Journal of Magnetism and Magnetic Materials*, vol. 320, no. 13. pp. 1904–1908.
- BUHL, S., SCHMIDT, K., SAPPOK, D., MERZ, R., GODARD, C., KERSCHER, E. and RIPPERGER, S. 2015. Surface structuring of case hardened chain pins by cold-sprayed microparticles to modify friction and wear properties. *Particuology*, vol. 21. pp. 32–40.
- CHENG, X., OUYANG, Y., SHI, H., ZHONG, X., DU, Y. and TAO, X. 2006. Nano-amorphous (FeAl)_{1-x}Zr_x alloys prepared by mechanical alloying. *Journal of Alloys and Compounds*, vol. 421, no. 1–2. pp. 314–318.
- CINCA, N., LIST, A., GÄRTNER, F., GULEMANY, J.M. and KLASSEN, T. 2015. Influence of spraying parameters on cold gas spraying of iron aluminide intermetallics. *Surface and Coatings Technology*, vol. 268. pp. 99–107.
- CODDET, P., VERDY, C., CODDET, C. and DEBRAY, F. 2015. Effect of cold work, second phase precipitation and heat treatments on the mechanical properties of copper–silver alloys manufactured by cold spray. *Materials Science and Engineering: A*, vol. 637. pp. 40–47.
- CODDET, P., VERDY, C., CODDET, C., DEBRAY, F., and LECOUTURIER, F. 2015. Mechanical properties of thick 304L stainless steel deposits processed by He cold spray. *Surface and Coatings Technology*, vol. 277. pp. 74–80.
- CONCUSTELL, A., HENAO, J., DOSTA, S., CINCA, N., CANO, I.G. and GULEMANY, J.M. (2015). On the formation of metallic glass coatings by means of Cold Gas Spray technology. *Journal of Alloys and Compounds*, vol. 651. pp. 764–772.
- COUPERTHWAITTE, R.A. and MWAMBA I.A. 2013. Effect of platinum group metal additions on the oxidation behaviour of Fe-40at.% Al. *Proceedings of the AMI 2013 Precious Metals Conference*, ISBN 978-1-920410-51-3. pp. 307–316
- COUPERTHWAITTE, R.A., CORNISH, L.A., MWAMBA, I.A. and PAPO, M.J. 2015. Effect of Processing Route on the Microstructure and Properties of an Fe-al Alloy with Additions of Precious Metal. *Materials Today: Proceedings*, vol. 2, no. 7. pp. 3932–3942.
- D'ANGELO, L., D'ONOFRIO, L. and GONZALEZ, G. 2009. Nanophase intermetallic FeAl obtained by sintering after mechanical alloying. *Journal of Alloys and Compounds*, vol. 483, no. 1–2. pp. 154–158.
- EELMAN, D., DAHN, J., MACKAY, G. and DUNLAP, R. 1998. An investigation of mechanically alloyed Fe–Al. *Journal of Alloys and Compounds*, vol. 266, no. 1–2. pp. 234–240.
- EHEMAM HAGHIGHI, S., JANGHORBAN, K. and IZADI, S. 2010. Order-sintering of mechanically alloyed FeAl nanostructures. *Journal of Alloys and Compounds*, vol. 503, no. 2. pp. 375–379.
- GRABKE, H. 1999. Oxidation of NiAl and FeAl. *Intermetallics*, vol. 7, no. 10. pp. 1153–1158.
- GRIGORIEV, S., OKUNKOVA, A., SOVA, A., BERTRAND, P. and SMUROV, I. 2015. Cold spraying: From process fundamentals towards advanced applications. *Surface and Coatings Technology*, vol. 268. pp. 77–84.
- GROSDIDIER, T., TIDU, A. and LIAO, H.-L. 2001. Nanocrystalline Fe-40Al coating processed by thermal spraying of milled powder. *Scripta Materialia*, vol. 44, no. 3. pp. 387–393.
- GUO, P., SHAO, Y., ZENG, C., WU, M. and LI, W. 2011. Oxidation characterization of FeAl coated 316 stainless steel interconnects by high-energy micro-arc alloying technique for SOFC. *Materials Letters*, vol. 65, no. 19–20. pp. 3180–3183.
- HENAO, J., CONCUSTELL, A., G.CANO, I., DOSTA, S., CINCA, N., GULEMANY, J.M. and SUHONEN, T. 2016. Novel Al-based metallic glass coatings by Cold Gas Spray. *Materials & Design*, vol. 94. pp. 253–261.
- HERRMANN-GEPPERT, I., BOGDANOFF, P., EMLER, T., DITTRICH, T., RADNIK, J., KLASSEN, T. and SCHIEDA, M. 2016. Cold gas spraying – A promising technique for photoelectrodes. *Catalysis Today*, vol. 260. pp. 140–147.
- JAKUPI, P., KEECH, P.G., BARKER, I., RAMAMURTHY, S., JACKLIN, R.L., SHOESMITH, D.W. and MOSER, D.E. 2015. Characterization of commercially cold sprayed copper coatings and determination of the effects of impacting copper powder velocities. *Journal of Nuclear Materials*, vol. 466. pp. 1–11.
- JAN, V., ČUPERA, J. and CIZEK, J. 2015. On the search for producing intermetallics by diffusion reaction of cold spray bulk deposits. *Surface and Coatings Technology*, vol. 268. pp. 216–223.
- JI, G., GORAN, D., BERNARD, F., GROSDIDIER, T., GAFFET, E. and MUNIR, Z.A. 2006. Structure and composition heterogeneity of a FeAl alloy prepared by one-step synthesis and consolidation processing and their influence on grain size characterization. *Journal of Alloys and Compounds*, vol. 420, no. 1–2. pp. 158–164.
- KEZRANE, M., GUITTOUM, A., BOUKHERROUB, N., LAMRANI, S., and SAHRAOUI, T. 2012. Mössbauer and X-ray diffraction studies of nanostructured Fe₇₀Al₃₀ powders elaborated by mechanical alloying. *Journal of Alloys and Compounds*, vol. 536. pp. S304–S307.

Cold-spray coating of an Fe-40 at.% Al alloy with additions of ruthenium

- KIM, K., LI, W. and GUO, X. 2015. Detection of oxygen at the interface and its effect on strain, stress, and temperature at the interface between cold sprayed aluminum and steel substrate. *Applied Surface Science*, vol. 357. pp. 1720–1726.
- KO, I.-Y., JO, S.-H., DOH, J.-M., YOON, J.-K. and SHON, I.-J. 2010. Rapid consolidation of nanostructured FeAl compound by high frequency induction heating and its mechanical properties. *Journal of Alloys and Compounds*, vol. 496, no. 1–2. pp. L1–L3.
- KOIVULUOTO, H., BOLELLI, G., MILANTI, A., LUSVARGHI, L. and VUORISTO, P. 2015. Microstructural analysis of high-pressure cold-sprayed Ni, NiCu and NiCu+Al₂O₃ coatings. *Surface and Coatings Technology*, vol. 268. pp. 224–229.
- KRASNOWSKI, M., GRABIAS, A. and KULIK, T. 2006. Phase transformations during mechanical alloying of Fe–50% Al and subsequent heating of the milling product. *Journal of Alloys and Compounds*, vol. 424, no. 1–2. pp. 119–127.
- KRASNOWSKI, M. and KULIK, T. 2007a. Nanocrystalline FeAl intermetallic produced by mechanical alloying followed by hot-pressing consolidation. *Intermetallics*, vol. 15, no. 2. pp. 201–205.
- KRASNOWSKI, M. and KULIK, T. 2007b. Nanocrystalline FeAl matrix composites reinforced with TiC obtained by hot-pressing consolidation of mechanically alloyed powders. *Intermetallics*, vol. 15, no. 10. pp. 1377–1383.
- KRASNOWSKI, M., WITEK, A. and KULIK, T. 2002. The FeAl–30%TiC nanocomposite produced by mechanical alloying and hot-pressing consolidation. *Intermetallics*, vol. 10, no. 4. pp. 371–376.
- KUC, D., NIEWIELSKI, G. and BEDNARCZYK, I. 2009. Structure and plasticity in hot deformed FeAl intermetallic phase base alloy. *Materials Characterization*, vol. 60, no. 10. pp. 1185–1189.
- LI, W.-Y., ZHANG, C., WANG, H.-T., GUO, X.P., LIAO, H.L., LI, C.-J. and CODDET, C. 2007. Significant influences of metal reactivity and oxide films at particle surfaces on coating microstructure in cold spraying. *Applied Surface Science*, vol. 253, no. 7. pp. 3557–3562.
- LUO, X.-T. and LI, C.-J. 2012. Dual-scale oxide dispersoids reinforcement of Fe–40at.%Al intermetallic coating for both high hardness and high fracture toughness. *Materials Science and Engineering: A*, vol. 555. pp. 85–92.
- LUO, X.-T. and LI, C.-J. 2015. Large sized cubic BN reinforced nanocomposite with improved abrasive wear resistance deposited by cold spray. *Materials and Design*, vol. 83. pp. 249–256.
- MASSALSKI, T.B. 1990. *Binary Alloy Phase Diagrams*, 2nd edn. vol. 1, ASM International. pp. 148–149.
- MONTEALEGRE, M.A., GONZÁLEZ-CARRASCO, J.L., MORRIS-MUÑOZ, M.A., CHAO, J. and MORRIS, D.G. 2000. The high temperature oxidation behaviour of an ODS FeAl alloy. *Intermetallics*, vol. 8, no. 4. pp. 439–446.
- NAYAK, S.S., WOLLGARTEN, M., BANHART, J., PABI, S.K. and MURTY, B.S. 2010. Nanocomposites and an extremely hard nanocrystalline intermetallic of Al–Fe alloys prepared by mechanical alloying. *Materials Science and Engineering: A*, vol. 527, no. 9. pp. 2370–2378.
- PALDEY, S. and DEEVI, S.C. 2003. Cathodic arc deposited FeAl coatings: properties and oxidation characteristics. *Materials Science and Engineering: A*, vol. 355, no. 1–2. pp. 208–215.
- SHI, H., GUO, D. and OUYANG, Y. 2008. Structural evolution of mechanically alloyed nanocrystalline FeAl intermetallics. *Journal of Alloys and Compounds*, vol. 455, no. 1–2. pp. 207–209.
- SKOGLUND, H., KNUTSON WEDEL, M. and KARLSSON, B. 2003. The role of oxygen in powder processing of FeAl. *Intermetallics*, vol. 11, no. 5. pp. 475–482.
- SKOGLUND, H., WEDEL, M.K. and KARLSSON, B. 2004. Processing of fine-grained mechanically alloyed FeAl. *Intermetallics*, vol. 12, no. 7–9. pp. 977–983.
- SONG, H., WU, Y., TANG, C., YUAN, S., GONG, Q. and LIANG, J. 2009. Microstructure and mechanical properties of FeAl intermetallics prepared by mechanical alloying and hot-pressing. *Tsinghua Science and Technology*, vol. 14, no. 3. pp. 300–306.
- VALDRÈ, G., BOTTON, G. and BROWN, L. 1999. High spatial resolution PEELS characterization of FeAl nanograins prepared by mechanical alloying. *Acta Materialia*, vol. 47, no. 7. pp. 2303–2311.
- WANG, H.-T., LI, C.-J., YANG, G.-J. and LI, C.-X. 2008a. Effect of heat treatment on the microstructure and property of cold-sprayed nanostructured FeAl/Al₂O₃ intermetallic composite coating. *Vacuum*, vol. 83, no. 1. pp. 146–152.
- WANG, H.-T., LI, C.-J., YANG, G.-J. and LI, C.-X. 2008b. Cold spraying of Fe/Al powder mixture: Coating characteristics and influence of heat treatment on the phase structure. *Applied Surface Science*, vol. 255, no. 5. pp. 2538–2544.
- XU, C., GAO, W. and GONG, H. 2000. Oxidation behaviour of FeAl intermetallics. The effects of Y and/or Zr on isothermal oxidation kinetics. *Intermetallics*, vol. 8, no. 7. pp. 769–779.
- XU, C.-H., GAO, W. and HE, Y.-D. 2000. High temperature oxidation behaviour of FeAl intermetallics—oxide scales formed in ambient atmosphere. *Scripta Materialia*, vol. 42, no. 10. pp. 975–980.
- XU, C.-H., GAO, W. and LI, S. 2001. Oxidation behaviour of FeAl intermetallics—the effect of Y on the scale spallation resistance. *Corrosion Science*, vol. 43, no. 4. pp. 671–688.
- YANG, G.-J., WANG, H.-T., LI, C.-J. and LI, C.-X. 2011. Effect of annealing on the microstructure and erosion performance of cold-sprayed FeAl intermetallic coatings. *Surface and Coatings Technology*, vol. 205, no. 23–24. pp. 5502–5509.
- YANG, Z.-G. and HOU, P.Y. 2005. Wrinkling behavior of alumina scales formed during isothermal oxidation of Fe–Al binary alloys. *Materials Science and Engineering: A*, vol. 391, no. 1–2. pp. 1–9.
- ZHU, X., YAO, Z., GU, X., CONG, W. and ZHANG, P. 2009. Microstructure and corrosion resistance of Fe–Al intermetallic coating on 45 steel synthesized by double glow plasma surface alloying technology. *Transactions of Nonferrous Metals Society of China*, vol. 19, no. 1. pp. 143–148. ◆